



Missouri University of Science and Technology
Scholars' Mine

Electrical and Computer Engineering Faculty
Research & Creative Works

Electrical and Computer Engineering

01 Oct 2006

Millimeter-Wave Differential Probe for Nondestructive Detection of Corrosion Precursor Pitting

Mohammad Tayeb Ahmad Ghasr

Missouri University of Science and Technology, mtg7w6@mst.edu

Brian D. Carroll

Sergey Kharkovsky

Missouri University of Science and Technology

Russell A. Austin

et. al. For a complete list of authors, see https://scholarsmine.mst.edu/ele_comeng_facwork/1728

Follow this and additional works at: https://scholarsmine.mst.edu/ele_comeng_facwork

 Part of the [Electrical and Computer Engineering Commons](#)

Recommended Citation

M. T. Ghasr et al., "Millimeter-Wave Differential Probe for Nondestructive Detection of Corrosion Precursor Pitting," *IEEE Transactions on Instrumentation and Measurement*, vol. 55, no. 5, pp. 1620-1627, Institute of Electrical and Electronics Engineers (IEEE), Oct 2006.

The definitive version is available at <https://doi.org/10.1109/TIM.2006.880273>

This Article - Journal is brought to you for free and open access by Scholars' Mine. It has been accepted for inclusion in Electrical and Computer Engineering Faculty Research & Creative Works by an authorized administrator of Scholars' Mine. This work is protected by U. S. Copyright Law. Unauthorized use including reproduction for redistribution requires the permission of the copyright holder. For more information, please contact scholarsmine@mst.edu.

Millimeter-Wave Differential Probe for Nondestructive Detection of Corrosion Precursor Pitting

Mohammad Tayeb Ghasr, *Member, IEEE*, Brian Carroll, *Student Member, IEEE*,
Sergey Kharkovsky, *Senior Member, IEEE*, Russell Austin, and Reza Zoughi, *Fellow, IEEE*

Abstract—Critical aircraft structural components, such as wings and fuselages, are exposed to harsh environments that vary considerably in temperature and moisture content. In most cases, the corrosion is hidden under paint and primer and cannot be visually detected. The initiation of corrosion is preceded by the presence of corrosion precursor pitting. Near-field millimeter-wave nondestructive testing (NDT) methods have been successfully used for detecting corrosion precursor pitting in exposed as well as painted aluminum substrates. However, near-field millimeter-wave measurements are susceptible to clutter that may mask indications of small defects such as pitting. Standoff distance variation produces an unwanted intensity gradient on an image and may be considered the most undesired clutter-producing effect. This paper presents a differential millimeter-wave probe consisting of a pair of radiating apertures. It is shown that the differential nature of this probe tends to significantly reduce the undesired effect of standoff distance variation, thereby enhancing probe detection sensitivity. Furthermore, when this probe is used for the purpose of millimeter-wave imaging, it produces defect indications with unique features that help in distinguishing the defect from noise. This dual differential probe was used for detecting corrosion precursor pitting. The design of the probe and the results of detecting various pittings are presented in this paper.

Index Terms—Corrosion, differential probe, millimeter waves, nondestructive testing (NDT), pits.

I. INTRODUCTION

CRITICAL aircraft structural components, such as wings and fuselages, are exposed to harsh environments that vary considerably in temperature and moisture content. These varied environmental conditions lead to corrosion of these components. In most cases, the corrosion is hidden under paint and primer and cannot be visually detected. Thus, detection is only possible when corrosion becomes severe and causes blistering of the paint. When this happens, a relatively large area must be rehabilitated, which may require significant time, resources, and downtime of the aircraft. The initiation of corrosion is preceded by the presence of corrosion precursor pitting. Detection

of precursor pitting yields information about the susceptibility to corrosion initiation [1]–[3]. The size (area and depth) of a precursor pitting is naturally very small (i.e., fractions of a millimeter); otherwise, when it becomes relatively large, the corrosion process has already started.

Near-field millimeter-wave nondestructive testing (NDT) techniques have been successfully used for detecting corrosion under thin and relatively thick dielectric coatings such as paint and composite materials [4]–[7]. Recently, near-field millimeter-wave NDT methods have also been successfully used for detecting corrosion precursor pitting in exposed as well as painted aluminum substrates [8], [9]. Near-field millimeter-wave NDT methods, using different types of probes such as open-ended rectangular waveguides, offer many advantages when inspecting complex composite structures [10]. However, all of these probes are susceptible to clutter, referred to any undesired signal, which masks indications of small defects such as pitting. The primary source of clutter in such measurements is standoff distance variation. Standoff distance is the distance between the aperture of a probe and a test specimen.

In this paper, the detection of pitting is represented by images that represent the severity and the spatial distribution of the pit. Such an image is produced by raster scanning a test specimen using an automated two-dimensional (2-D) scanning table that moves the specimen underneath a probe held at a fixed standoff distance above it. Raster scanning produces a 2-D matrix consisting of measured data (commonly a dc voltage [10]) proportional to the local reflection properties of the specimen. These voltages are then normalized with respect to the dynamic range of the entire collected data, and different grayscale levels are assigned to them, resulting in a corresponding image of the scanned area. An image produced in this way provides information about relative signal variation in that image only, and the same two grayscale levels in two different images do not correspond to the same detected voltage values [10]. Therefore, in some cases when two images need to be compared, their matrices can be augmented first, and then, the new matrix is normalized, and a new image is produced. In this way, the voltage outputs in different regions of the original two images scan can be directly compared.

When raster scanning an area for the purpose of imaging corrosion pitting, a few tens of micrometers change in standoff distance across an image may totally mask pitting indications, consequently making real-time imaging practically impossible

Manuscript received August 8, 2005; revised March 13, 2006. This work was supported by an Air Force Phase II SBIR grant.

M. T. Ghasr, B. Carroll, S. Kharkovsky, and R. Zoughi are with the Applied Microwave Nondestructive Testing Laboratory, Electrical and Computer Engineering Department, University of Missouri–Rolla, Rolla, MO 65409 USA (e-mail: zoughir@umr.edu).

R. Austin is with Texas Research Institute at Austin, Austin, TX 78733-6201 USA.

Digital Object Identifier 10.1109/TIM.2006.880273

for this purpose. If the standoff distance is measured, then by knowing the relationship between the standoff distance and the output of the probe, one could compensate for the adverse effect of standoff distance change. Compensation is referred to as removing or reducing the effect of standoff distance change from the output of the probe (i.e., the probe output should be independent of standoff distance and should be only dependent on the reflection properties of the specimen under test). To reduce the effect of standoff distance variation, Qaddoumi *et al.* [11] used a distance meter utilizing a potentiometer that attaches to the side of the probe, and while scanning, the change in the standoff distance is continuously measured, and its effect on the probe output voltage is subsequently removed. This method, albeit effective in removing adverse effect of standoff distance variation, suffers from several limitations.

- The potentiometer tip is always in contact with the specimen under test.
- Compensation is based on the standoff distance at the side of the probe and not directly beneath the probe aperture.
- Compensation dynamic range is small (only a linear region of less than quarter wavelength), and it increases probe sensitivity to standoff distance change outside this region.
- It requires calibration.

The primary objective of this investigation has been to detect very small corrosion pitting under paint while keeping the adverse influence of clutter (most notably standoff distance variation) to a minimum. Additionally, the measurement requirements call for a rapid, noncontact, and robust system. Consequently, to achieve these goals while eliminating most of the limitations in the previous standoff distance variation removal approach [11], the design and development of a dual differential approach was undertaken. This paper presents the design and testing of a dual differential probe consisting of a pair of identical probing apertures that, when utilized in tandem, significantly reduce the adverse effect of standoff distance variation while overcoming most of the limitations associated with the approach mentioned above. This dual differential probe has many other advantages such as being small and portable for on-site measurements. As will be seen later, millimeter-wave images of small pitting were produced using the dual differential probe. These images exhibit unique features that indicate the effectiveness of this probe as a real-time NDT tool.

II. DUAL DIFFERENTIAL PROBE

A. Design and Principle of Operation

The basic schematic of the dual differential probe is shown in Fig. 1. This probe consists of a millimeter-wave source, a magic tee (hybrid coupler), two identical waveguide aperture probes, and a detector. A continuous-wave (CW) oscillator such as a Gunn oscillator is used to generate a signal in the V-band frequency range (50–75 GHz), which is then fed to the sum (Σ) port of the magic tee through an isolator that prevents unwanted reflections from entering the oscillator. The magic tee serves two purposes. First, it divides the signal from the oscillator into two equal in-phase and magnitude signals at its colinear arms, each of which is connected to identical open-

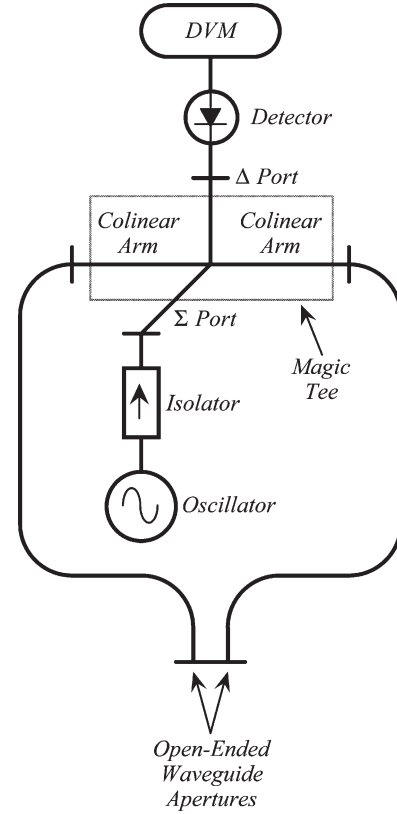


Fig. 1. Basic schematic of the dual differential probe.

ended rectangular waveguide aperture probes via two identical transmission lines. These aperture probes, when placed over a specimen under test, irradiate localized and immediate areas beneath them and pickup reflected signals from the specimen. These reflected signals subsequently travel back to the magic tee through the same two transmission lines.

The second purpose of the magic tee is to redirect the two reflected signals from each probe aperture to the detector. If the two reflected signals are labeled S_1 and S_2 , the magic tee will generate $0.5(S_1 + S_2)$ at its sum port, which is then absorbed by the isolator. On the other hand, the difference of the reflected signals $0.5(S_1 - S_2)$ appears at the difference (Δ) port of the magic tee and is subsequently fed to the diode detector, resulting in a dc voltage measured by a digital voltmeter (DVM). This voltage represents the difference between the reflected signals measured by each aperture probe.

Since the two waveguide apertures of the dual differential probe are adjacent to each other, the dual differential probe senses the difference between reflected signals from close-to-each other areas on the test specimen. While scanning a test specimen, if the two reflected signals are identical in magnitude and phase (e.g., the two waveguide apertures are probing areas with identical features), then the input signal to the detector will be zero (i.e., coherent difference between these two reflected signals), resulting in no detector output voltage. However, when one of the waveguide apertures senses a small localized target such as a pitting, the signal input to the detector will no longer be zero, and the detector produces a voltage proportional to the magnitude of the difference signal.

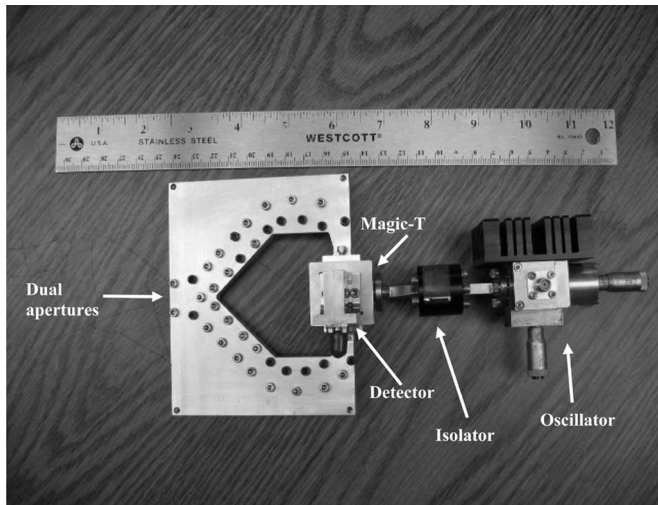


Fig. 2. Realization of the dual differential probe at V-band.

The effectiveness of this dual differential probe in removing the adverse effect of standoff distance variation is illustrated here since variation in standoff distance affects both apertures equally, resulting in no change in the output of the dual differential probe.

Ideally, the dual differential probe should not be affected by standoff distance variation no matter how severe this variation may be. However, the qualities of commercially available components, such as the magic tee, influence the ultimate practical response of this probe to standoff distance variation. The response of the dual differential probe to standoff distance variation will be discussed later. It must be mentioned that half of the power from each reflected signal is absorbed by the isolator at the sum port. Although this may be considered a negative issue, usually, commercial diode detectors are very sensitive, and only a relatively small signal level at the detector is required to produce a detectable output voltage. Therefore, a 3-dB loss of the signal does not have a significant undesired effect on the measurements as long as there is adequate power associated with the difference signal appearing at the detector.

B. Removal of Standoff Distance Variation

A V-band prototype of the dual differential probe is shown in Fig. 2. The waveguide section connecting the magic tee to the dual waveguide apertures were machined out of a block of aluminum. The terminal ends of these waveguide sections were then used as the open-ended rectangular waveguide probe apertures. This dual differential probe was used to produce the results presented in this paper. However, first, it is necessary to compare the output signal characteristics of this dual differential probe and a single probe as a function of standoff distance. In this investigation, the single probe is referred to a system that has similar circuitry to the dual differential probe (oscillator, magic tee, and detector), where one of the collinear arms is connected to the open-ended rectangular waveguide (the probing aperture), and the other is connected to a fixed reference (i.e., short circuit or a matched load). Fig. 3 shows the responses of a V-band single probe and the dual differential probe to standoff

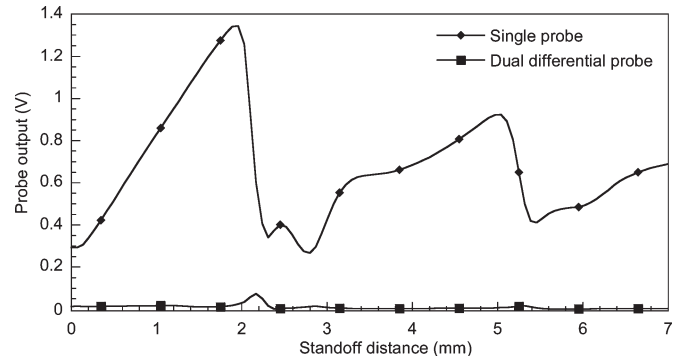


Fig. 3. Comparison between the V-band typical single-probe standoff distance response and that obtained using a dual differential probe at 67 GHz.

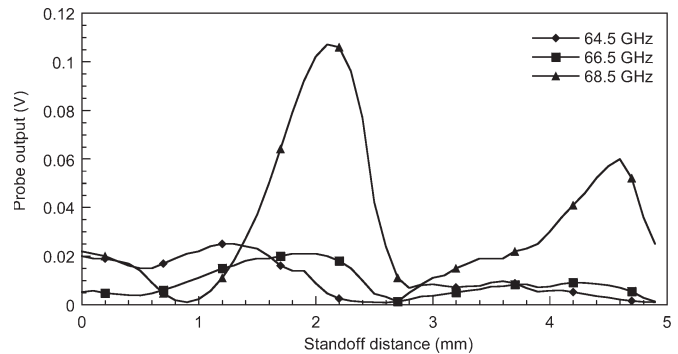


Fig. 4. Response of the V-band dual differential probe to standoff distance variation at three frequencies.

distance change when irradiating a flat aluminum plate. As expected, the single probe produced a changing voltage in the range 300–1400 mV as a function of increasing standoff distance. On the other hand, the dual differential probe produced a fairly flat response at around 10 mV, except at distances equal to multiples of half wavelength. These small peaks are due to the fact that the system is not totally balanced. Therefore, sharp changes in the signal, such as the 180° phase jump at every half wavelength, cause these peaks to appear. Balance of the dual differential probe depends on three factors, namely 1) the characteristics of the magic tee, 2) the waveguide sections connecting to its collinear ports, and 3) the probing apertures. For the dual differential probe to be balanced, the two apertures as well as the two waveguide sections should be identical. Furthermore, if the signal at the collinear ports of the magic tee are labeled S_1 and S_2 , then the signals at the sum port will be $a_1 S_1 + a_2 S_2$, and at the difference port, the signal is $a_1 S_1 - a_2 S_2$. If $a_1 = a_2$, then the magic tee is balanced (i.e., ideally $a_1 = a_2 = 0.5$).

Since the pittings of interest are very small, small standoff distances of less than 2 mm were used while producing images of a pitting using this V-band dual differential probe. At these small distances, the output of a single probe changes by more than 0.5 mV for every micrometer of standoff distance change, whereas the changes in the output of a dual differential probe are negligible, as shown in Fig. 3. Considering the fact that the signal dynamic range obtained for pitting of interest does not exceed a few tens of millivolts, standoff distance change of few micrometers can easily mask the image of a pitting.

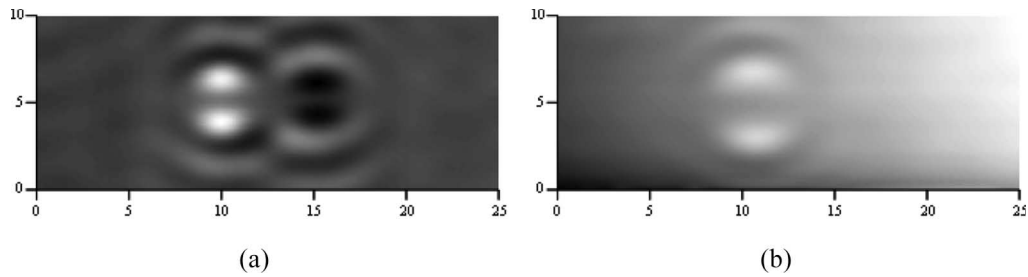


Fig. 5. Millimeter-wave images of a small piece of clear tape on an aluminum plate at 67 GHz using (a) dual differential probe and (b) single probe.

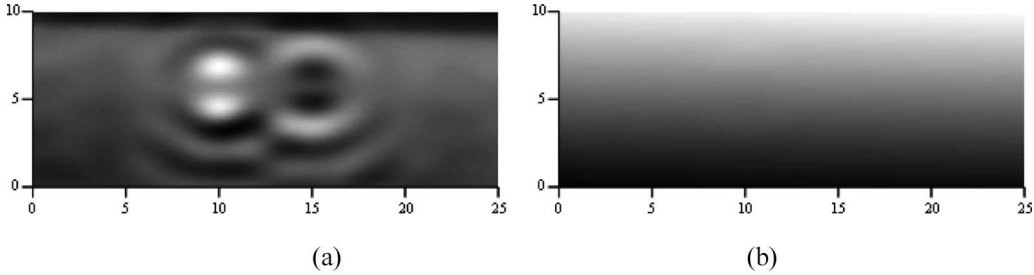


Fig. 6. Millimeter-wave images of a small piece of clear tape on a slanted aluminum plate at 67 GHz using (a) dual differential probe and (b) single probe.

As mentioned earlier, the performance of the dual differential probe is highly dependent on the quality of the components used to construct it. It is difficult to obtain components that have flat response at all frequencies within a given band. Fig. 4 shows the response of the dual differential probe (as shown in Fig. 2) to standoff distance variation at several frequencies. Clearly, a change of ± 2 GHz around 66.5 GHz affects the performance of the dual probe significantly. This V-band prototype was experimentally determined to have good overall performance at 67 GHz. Therefore, all of the results presented in this paper are obtained at this frequency.

The following experiment was performed to demonstrate the ability of dual differential probe in removing the effect of standoff distance change when producing an image. A small patch of clear tape ($1 \times 1 \times 0.1$ mm in dimensions) was placed on an aluminum plate and scanned using the dual differential and a single probe. This patch of tape is difficult to detect since it is very thin, spatially small, and expected to have similar reflection properties to a thin layer of corrosion (i.e., similar dielectric properties). First, the aluminum plate was placed flat on the scanning table and raster scanned. The resulting images for the tape are shown in Fig. 5. Fig. 5(a) shows the image obtained by the dual differential probe. As expected, the background of the image is very clear and does not show any traces of clutter. This image shows two horizontally spaced indications of opposite intensities (dark and bright). The distance between the two indications is 7 mm, which corresponds to the distance between the two probing apertures. During the scanning process, each time one of the probing apertures comes over the tape, an indication is registered in the image. Since the dual differential probe is utilizing two probing apertures, two indications for the tape are obtained. These two indications have opposite intensities due to the fact that, from the detector's point of view, the two probing apertures are 180° out of phase. Each of the two indications shows features similar to those obtained using open-ended rectangular waveguide apertures [9]. These

features include the spots in the middle of each indication and the surrounding rings. On the other hand, in the image obtained using the single probe [Fig. 5(b)], the contrast appears to be significantly lower (i.e., the image looks rather faint) since the probe was affected by a slight standoff distance change appearing as a gradient of intensity change across (from left to right) the image.

In another experiment, the aluminum plate was slanted, resulting in a standoff distance change of 2 mm across the scanned area. The specimen was scanned again using the dual differential and the single probe, and the resultant images are shown in Fig. 6. As expected, the dual differential probe was negligibly affected by this standoff distance changes, as shown in Fig. 6(a). The background of the image is fairly uniform, showing minimal effect of varying standoff distance. More importantly, the two indications with opposite intensities are still clearly visible in this image. On the other hand, the image obtained using the single probe [Fig. 6(b)] shows that the probe was severely affected by the changing standoff distance, and subsequently, there is no indication of the tape in this image compared with the image shown in Fig. 5(b).

C. Other Clutter Sources

In addition to changes in standoff distance, there are other clutter sources that may potentially mask indications of small defects. Due to the dual probe's differential nature, any clutter source that affects both of the probing apertures equally will not be registered in the resulting image. Some of these clutter sources are as follows: sharp edges on the specimen under test, paint thickness variation, and oscillator instability. Variation in the thickness of a dielectric coating such as paint has a similar effect as variation in standoff distance. If paint thickness changes in an area larger than the combined area of the dual differential probe apertures, both apertures will register the same change. Hence, the final output will not be affected.

Oscillator power or frequency instability, which may be caused by changes in the temperature or changes in the oscillator bias voltage, may cause significant undesired changes in the output of a single probe. However, the dual differential probe eliminates these variations since they affect both probes equally. A variation in the output power of the oscillator changes the sensitivity of the dual probe to the presence of defects by changing the amount of power radiated onto the specimen and subsequently reflected back from it. However, unless this variation is a significant decrease in the oscillator power, any resulting adverse effect is negligible. The effect of frequency change in the oscillator on the performance of the dual differential probe is dictated by the frequency response of the components used in its construction such as the magic tee. Practically, it is difficult to build components that have a flat frequency response throughout V-band. However, small changes in the frequency of operation, for example, changes of less than 0.5 GHz at V-band, have minimal consequences. Furthermore, oscillators that are stable to within these limits are relatively easy to obtain commercially.

Another clutter source that single probes suffer from is edge effect associated with physical edges of the specimen under test such as weld and lap joints. Edge effect causes standing wave pattern on the specimen and is subsequently manifested by interference lines appearing in an image. These lines are parallel to the edges of a panel and are spaced by half of a wavelength [12]. Edge effect is accentuated if the metal substrate is covered by a thin dielectric coating such as paint. Thin dielectric coatings such as paint promote the presence of surface wave on the panel [9].

Since the electric field in a rectangular waveguide is linearly polarized, only edges that are orthogonal to the electric field polarization cause interference in the image. In the case of the dual differential probe, if the two probing apertures are at the same electrical distance from the edge, the interference from the edge is automatically cancelled. To maintain the same electrical distance from the probing aperture to the edge, two cases may be considered. If the probing apertures are joined from their narrow walls, then the dual differential probe should be placed such that the edge is parallel to the broad wall of the probing apertures. If the two probing aperture are joined by their broad walls, then the distance between the centers of the probing apertures should be $\lambda/2$, where λ is the wavelength. In the case where the edge is not orthogonal to the electric field, then the dual differential probe may reduce or boost the influence of edge effect depending on the angle between the probing apertures and the edge. All that said, it is fairly easy to observe the presence of an edge on a panel under test and fix the orientation of the dual differential probe accordingly.

III. PITTING DETECTION

Several aluminum panels containing pitting of various sizes and properties were produced for this investigation. One 3-mm-thick aluminum panel was placed in a salt fog chamber to produce natural pitting. The second aluminum panel had three sets of identical laser-machined pittings with openings (diameters) and depths ranging from 100 to 500 μm . One set of pittings

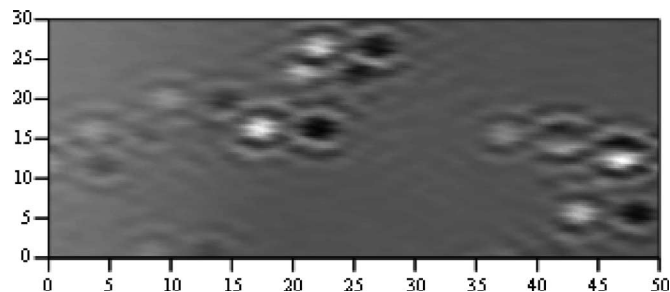


Fig. 7. Image of the naturally pitted sample obtained using the V-band dual differential probe at 67 GHz.

was left exposed, whereas the other two sets were covered by a thin layer of paint and appliqué (paint-like polymer), respectively. The third aluminum panel had three exposed sets of laser-machined pittings with depths and diameters in the range of 200–400 μm with several different spacing between the pittings. In one set, the pittings were spaced 6 mm apart, and in the other two, the spacing was 12 and 20 mm.

Fig. 7 shows the dual probe image of an area on the first panel containing natural pitting under three layers of clear tape simulating paint. Unlike the case of a single probe where the spatial resolution of the probe depends only on the type of probe, the spacing between the apertures in a dual differential probe is also an important factor influencing the spatial resolution. The spacing between the apertures is a function of the aperture dimensions. Larger apertures will be spaced further apart than smaller apertures. Pittings that are spaced less than the spacing between the dual probe apertures will not be represented with separate indications. This fact is illustrated in Fig. 7, where closely packed pittings produce images that merge together. This is not a major issue from the detection point of view since larger pittings will dominate the detection scene, and detections of smaller pitting in the close proximity of large pittings become significantly less critical.

Fig. 8 shows the image of three laser-machined pittings under appliqué (second panel) with diameters of 500 μm and depths of 150, 200, and 500 μm . This image shows the three pittings in the form of dual indications of opposite intensities with a clear background, as expected. This image represents the raw data obtained from the dual differential probe without any signal or image processing. These pittings were previously imaged using a single probe, where the image was severely affected by the presence of edge effect [9]. Fig. 9 shows the image of a laser-machined pitting with a diameter of 150 μm and depth of 500 μm under paint. In this image, the background does not seem to be as uniform as in the previous images. This is due to the variations in the paint thickness, especially around the pit. Since this plate was painted after the pits were laser machined, more paint concentrated around the pit. The dual differential probe senses some of these paint variations since they are localized. However, the unique indication produced by the dual probe (dual indications of opposite intensities) stands out from all other clutter in the image. This fact reduces the chances of missing a defect or the number of false indications.

The capability of the dual differential probe to reduce clutter is not affected by the type of probing apertures as long as they

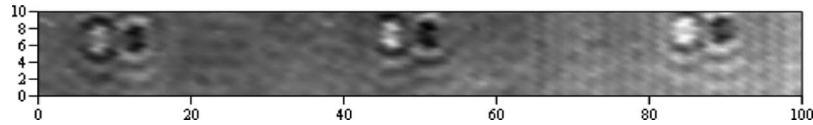


Fig. 8. Image of three pits 500 μm in diameters and depths of (from left to right) 150, 200, and 500 μm under appliqué obtained at 67 GHz using the V-band dual differential probe.

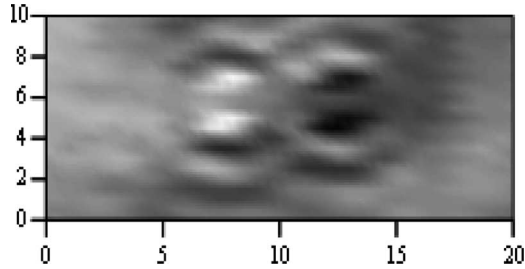


Fig. 9. Image of a 150- μm -deep and 500- μm -diameter pit under paint obtained using the V-band dual differential probe operating at 67 GHz.

are identical. However, the detection sensitivity of the dual differential probe is directly related to the type and characteristics of probing apertures used with the dual differential probe. One type of the probing apertures that enhances the detection sensitivity of a millimeter-wave system is a dielectric waveguide probe. The dielectric waveguide is made out of a low-loss dielectric material with high permittivity (e.g., a ceramic with $\epsilon_r = 9.8$). The dielectric waveguide is made into a slab with equal height to that of the narrow dimension of a rectangular waveguide. The optimum width of the dielectric slab was determined to be 13% of the broad dimension of the rectangular waveguide [9]. One end of the dielectric slab was inserted into the rectangular waveguide to couple the signal from and to the slab. The other end, which has a much smaller aperture than the open-ended rectangular waveguide (the commonly used probing aperture), was used as the probing aperture. Consequently, the electromagnetic field concentrates mainly at the aperture of the dielectric slab, which results in a sensitive and high-resolution probe [9]. Two identical dielectric slabs were made and used as probing apertures with the dual differential probe. Fig. 10 shows an image of a set of laser-machined pittings with diameter and depth in the range 200–400 μm (third panel) obtained using the V-band dual differential probe with dielectric waveguides as probing apertures. In this image, the dual inverse indication, which is a signature of the dual differential probe, is preserved. Furthermore, pitting indications do not have rings associated with them and appear as a single spot (features of a dielectric waveguide aperture [9]). Except for the smallest of these pittings (200 μm in diameter and depth), all of these pittings are visible.

IV. SUMMARY AND DISCUSSION

Near-field millimeter-wave techniques are powerful tools for the purpose of detecting corrosion precursor pittings under paint. Traditional near-field millimeter-wave probes suffer from effects of clutter such as standoff distance variation that

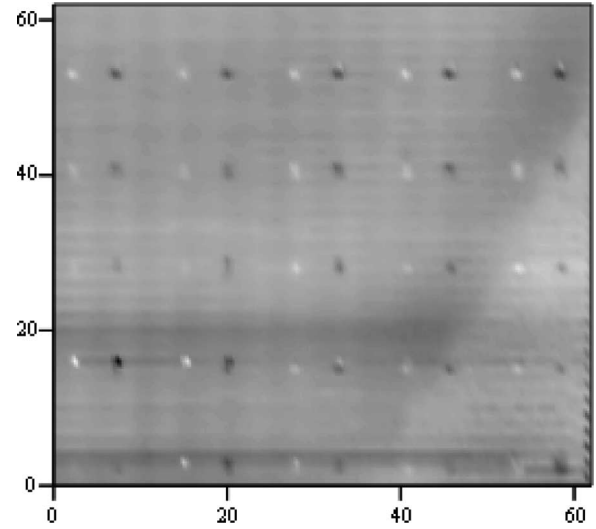


Fig. 10. Image of a set of pits 200–400 μm in diameter and depth obtained using a V-band dual differential probe operating at 67 GHz and employing dielectric waveguide probes.

severely limit their detection capabilities. The output of the dual differential probe is the coherent difference between the reflection properties of two closely spaced areas on the sample under test. Therefore, the effect of clutter such as standoff distance variation is inherently removed from the output. This probe is also stable against any changes in temperature that lead to oscillator instability.

The overall performance of the dual differential probe is governed by the quality of components used to construct it, in particular, the magic tee. The balance of the magic tee depends on the frequency of operation. Even full-band magic tees do not have a constant balance throughout the band. The V-band dual differential probe was found to be fairly balanced at 67 ± 0.5 GHz.

Since the dual differential probe is not affected by standoff distance change or any other clutter source, real-time imaging becomes more feasible. The images produced by the dual probe will not require any postprocessing to enhance the detection schemes. Moreover, the unique signature of the dual differential probe (i.e., the dual indication with opposite intensities) makes identifying pittings from noise fairly easy. Basically, one should look for bright and dark indications with a known spacing (spacing of apertures) in the image.

The dual differential probe was used to image natural and laser-machined pitting exposed and under paint. By reducing the effect of standoff distance variation and other clutter sources, the dual differential probe produced images of these pittings with high contrast. The unique features of the

indications help in identifying the pittings from other anomalies that may be present on the image. The spatial resolution of the probe depends significantly on the footprint of the probing aperture used. If the footprint of the probing aperture is larger than the spacing between the pittings, then their respective indications will be combined in the image. Using dielectric waveguides, the spatial resolution and detection sensitivity of the dual differential probe are increased without sacrificing its clutter removing performance.

REFERENCES

- [1] R. Baboian, Ed., *Corrosion Tests and Standards: Application and Interpretation*. Philadelphia, PA: Ameri. Soc. Testing Materials, 1995.
- [2] W. Funke, "Blistering of paint films," in *Corrosion Control by Organic Coatings*, H. Leidheiser, Jr., Ed. Houston, TX: Nat. Assoc. Corrosion Eng., 1981, pp. 97–102.
- [3] J. A. Collins, *Failure of Materials in Mechanical Design*, 2nd ed. New York: Wiley, 1993.
- [4] W. C. Fitzgerald, M. N. Davis, J. L. Blackshire, J. F. Maguire and D. B. Mast. (2001). Evanescent microwave sensor scanning for detection of sub-coating corrosion. *J. Corros. Sci. Eng.* [Online]. 3, Paper 15. Available: <http://www.jcse.org/Volume3/Paper15/v3p15.html>
- [5] N. Qaddoumi, A. Shroyer, and R. Zoughi, "Microwave detection of rust under paint and composite laminates," *Res. Nondestruct. Eval.*, vol. 9, no. 4, pp. 201–212, 1997.
- [6] N. Qaddoumi, L. Handjojo, T. Bigelow, J. Easter, A. Bray, and R. Zoughi, "Microwave corrosion detection using open-ended rectangular waveguide sensors," *Mater. Eval.*, vol. 58, no. 2, pp. 178–184, Feb. 2000.
- [7] D. Hughes, N. Wang, T. Case, K. Donnell, R. Zoughi, R. Austin, and M. Novack, "Microwave nondestructive detection of corrosion under thin paint and primer in aluminum panels," *Special Issue Subsurf. Sens. Technol. Appl.: Adv. Appl. Microw. Millimeter Wave Nondestruct. Eval.*, vol. 2, no. 4, pp. 435–451, 2001.
- [8] D. Hughes, R. Zoughi, R. Austin, N. Wood, and R. Engelbart, "Near-field microwave detection of corrosion precursor pitting under thin dielectric coatings in metallic substrates," in *Proc. 29th Annu. Rev. Progress Quant. Nondestruct. Eval.*, Bellingham, WA, Jul. 14–19, 2002, vol. 22B, pp. 462–469.
- [9] M. Ghasr, S. Kharkovsky, R. Zoughi, and R. Austin, "Comparison of near-field millimeter wave probes for detecting corrosion pit under paint," in *Proc. IEEE IMTC*, Como, Italy, May 18–20, 2004, pp. 2240–2244.
- [10] R. Zoughi, *Microwave Non-Destructive Testing and Evaluation*. Dordrecht, The Netherlands: Kluwer, 2000.
- [11] N. Qaddoumi, T. Bigelow, R. Zoughi, L. Brown, and M. Novack, "Reduction of sensitivity to surface roughness and slight standoff distance variation in microwave testing of thick composite structures," *Mater. Eval.*, vol. 60, no. 2, pp. 165–170, Feb. 2002.
- [12] N. Qaddoumi, "Microwave detection and characterization of sub-surface defect properties in composites using an open-ended rectangular waveguide," Ph.D. dissertation, Elect. Comput. Eng. Dept., Colorado State Univ., Fort Collins, CO, 1998.



Brian Carroll (S'04) received the B.S.E.E. degree from the University of Missouri–Rolla (UMR) in 2005. He is currently working toward the M.S.E.E. degree at the same university.

Since 2004, he has done undergraduate- and graduate-level research with the Applied Microwave Nondestructive Testing Laboratory, Electrical and Computer Engineering Department, UMR.



Sergey Kharkovsky (M'00–SM'03) received the M.S. degree in electronics engineering from Kharkov Institute of Radioelectronics, Kharkov, Ukraine, in 1975, the Ph.D. degree in radiophysics from Kharkov State University in 1985, and the D.Sc. degree in radiophysics from the Institute of Radiophysics and Electronics (IRE), National Academy of Sciences of Ukraine, Kharkov, in 1994.

Currently, he is a Research Associate Professor with the Electrical and Computer Engineering Department, University of Missouri–Rolla (UMR).

Prior to joining UMR, he was a member of the Research Staff at IRE from 1975 to 1998. From 1998 to 2002, he was a Professor with the Electrical and Electronics Engineering Department, Cukurova University, Adana, Turkey. He was a Visiting Associate Professor with the Electrical and Computer Engineering Department, UMR, from March 2003 to February 2006. His research area with IRE was the investigation and development of new millimeter-wave techniques, including dielectric resonators with whispering gallery modes, solid-state oscillators, and their application for material characterization. His current research interest is nondestructive testing and evaluation of composite structures using microwaves and millimeter waves.



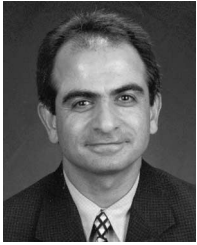
Mohammad Tayeb Ghasr (M'01) received the B.S.E.E. degree from the American University of Sharjah, Sharjah, U.A.E., in 2002 and the M.S.E.E. degree from the University of Missouri–Rolla (UMR) in 2004.

Since 2003, he has been a Graduate Research Assistant with the Applied Microwave Nondestructive Testing Laboratory, Electrical and Computer Engineering Department, UMR. His current research involves millimeter-wave imaging and the detection of corrosion and corrosion precursor pitting in aircraft structures using microwave- and millimeter-wave nondestructive testing techniques.

aircraft structures using microwave- and millimeter-wave nondestructive testing techniques.

Russell Austin received the B.S. degree in materials engineering from the New Mexico Institute of Mining and Technology, Socorro.

He is the Nondestructive Testing (NDT) Division Head with Texas Research Institute, Austin, where he has worked since 1993. Previously, he spent two years with the NDT group at Argonne National Laboratories, Argonne, IL. He has written numerous papers, coauthored two books, and has two patents pending. His primary research areas are ultrasonic, acoustic emission, and microwave NDT. He is also involved in embedded systems for continuous health monitoring of structures and aircraft.



Reza Zoughi (S'85–M'86–SM'93–F'06) received the B.S., M.S., and Ph.D. degrees in electrical engineering (radar remote sensing, radar systems, and microwaves) from the Radar Systems and Remote Sensing Laboratory, University of Kansas, Lawrence, in 1982, 1983, and 1987, respectively.

Currently, he is the Schlumberger Distinguished Professor of electrical and computer engineering with the University of Missouri–Rolla (UMR). Prior to joining UMR in January 2001 and since 1987, he was with the Electrical and Computer Engineering Department, Colorado State University (CSU), Fort Collins, where he was a Professor, and established the Applied Microwave Nondestructive Testing Laboratory. He held the position of Business Challenge Endowed Professor of electrical and computer engineering from 1995 to 1997 while at CSU. He has to his credit over 350 journal publications, conference proceedings and presentations, technical reports, and overview articles. He is also the author of a graduate textbook entitled *Microwave Nondestructive Testing and Evaluation Principles* (Boston, MA: Kluwer, 2000) and the coauthor, with A. Bahr and N. Qaddoumi, of a chapter on Microwave Techniques in an undergraduate introductory textbook entitled *Nondestructive Evaluation: Theory, Techniques, and Applications* (New York: Marcel Dekker, 2002). He has seven patents to his credit, all in the field of microwave nondestructive testing (NDT) and evaluation. His current areas of research include developing new NDT for microwave and millimeter-wave inspection and testing of materials, developing new electromagnetic probes to measure characteristic properties of material at microwave frequencies, and developing embedded modulated scattering techniques for NDT purposes, in particular for complex composite structures.

Dr. Zoughi is a Fellow of the American Society for Nondestructive Testing (ASNT). He is the Associate Editor-in-Chief for the IEEE TRANSACTIONS ON INSTRUMENTATION AND MEASUREMENT, the Editor for *Research in Nondestructive Evaluation*, the Technical Associate Editor for *Materials Evaluation*, the Guest Associate Editor for the Special Microwave NDE Issue of *Research in Nondestructive Evaluation* in 1995, and the Co-Guest Editor for the Special Issue of *Subsurface Sensing Technologies and Applications: Advances and Applications in Microwave and Millimeter Wave Nondestructive Evaluation*. He served as the Research Symposium Co-Chair for the ASNT Spring Conference and the 11th Annual Research Symposium, Portland, OR, in March 2002, and as the Technical Chair for the IEEE Instrumentation and Measurement Technology Conference (IMTC2003), Vail, CO, in May 2003. He served as the Guest Editor for the IMTC2003 special issue of the IEEE TRANSACTIONS ON INSTRUMENTATION AND MEASUREMENT. In the past five years at UMR, he has received two Outstanding Teaching Commendations, two Outstanding Teaching Awards, and two Dean of Engineering Excellence in Teaching Awards. He was voted the most outstanding teaching faculty seven times by the junior and senior students at the Electrical and Computer Engineering Department, CSU. He received the College of Engineering Abell Faculty Teaching Award in 1995. He is the 1996 recipient of the Colorado State Board of Agriculture Excellence in Undergraduate Teaching Award (only one faculty recognized for this award at each of the three CSU system campuses). He was recognized as an honored researcher for seven years by the Colorado State University Research Foundation. He has given numerous invited talks on the subject of Microwave Nondestructive Testing and Evaluation. He is also a member of Sigma Xi and Eta Kappa Nu.